ELSEVIER

Catalysis Today 48 (1999) 131–138

CATALYSIS TODAY

Gas–solid adhesion and solid–solid agglomeration of carbon supported catalysts in three phase slurry reactors

M. van der Zon*, P.J. Hamersma, E.K. Poels, A. Bliek

Department of Chemical Engineering, University of Amsterdam, Nieuwe Achtergracht 166, 1018 WV Amsterdam, Netherlands

Abstract

In the study of three phase slurry reactors the slurry phase is conventionally treated as a quasi homogeneous liquid phase with altered sorption and reaction capacity due to the presence of catalyst particles. This approach may be utterly wrong in any case where phase segregation of the solid takes place. This phenomenon is relatively little studied and it will be demonstrated that it may have a considerable impact on the operation of three phase reactors. Two examples of segregation, i.e. gas–solid adhesion and solid–solid agglomeration, are to be discussed. Taking the example of carbon and alumina supported palladium catalysts employed in the hydrogenation of methyl acrylate towards methyl propionate, the segregation of the catalyst phase by adhesion to gas bubbles is studied. This adhesion may take place up to complete coverage of the gas bubbles but it may also be entirely absent. A quantitative model is developed based on the film theory, the particle to bubble collision probability and the impact of the size of adhering particles on the effective film thickness. This model is used to describe adhesion under non-stagnant conditions and the impact it has on the overall G–L mass transfer rates. The conversion rate of a mass transfer limited model reaction, i.e. the hydrogenation of methyl acrylate to methyl propionate, is studied in a stirred tank reactor for two different catalysts (Pd/C and Pd/Al_2O_3) in order to verify the model. It is quantitatively demonstrated that G–L mass transfer rates may be increased considerably as a result of adhesion. The second, closely related, phenomenon studied is the segregation of the solid and liquid phase by agglomeration of the catalyst particles. This behaviour is of particular importance as it leads to a substantial increase in the effective particle size resulting in a decreased conversion rate.

Keywords: Pd/C; Hydrogenation; Slurry reactor; Adhesion; Agglomeration; Mass transfer

1. Introduction

Three phase slurry reactors are widely used in chemical and biochemical industries. In most of these reactors a catalyst is present as a dispersed solid phase. The effect of the presence of catalyst particles on the hydrodynamic behaviour of a three phase slurry reactor, either on the mass transfer rate of the gaseous reactant to the catalyst surface or on the coalescence of bubbles, is still not well understood. In this paper we will focus on the effect of two types of segregation phenomena, agglomeration and adhesion of catalyst particles, on the mass transfer processes and the conversion rate of the key component.

The conversion rate of a gas–liquid mass transfer limited reaction may be enhanced by the presence of small catalyst particles adhering to gas bubbles. Vinke et al. [1] showed with bubble pick up experiments that small hydrophobic particles will adhere to bubbles in an aqueous slurry, while hydrophilic particles do not.

*Corresponding author.

0920-5861/99/$ – see front matter
PII: S0920-5861(98)00367-8

This adhesion may either affect the mass transfer rate by an increasing specific bubble surface a_L and/or by an increasing mass transfer coefficient k_L. According to Lindner et al. [2] the main reason for mass transfer enhancement is the increase of a_L, caused by a decreasing bubble coalescence rate. Other authors suggest an increase of the value of k_L. Alper et al. [3], Kars et al. [4], Quicker et al. [5] introduced the so called grazing or shuttle effect, where it is assumed that particles, smaller than the liquid side film thickness, penetrate into the gas–liquid boundary layer. Because of the high gas concentration in this layer compared to the bulk liquid, the adsorption rate from the gas phase increases. Saturated catalyst particles can move back into the bulk liquid and increase the gas phase concentration there.

The model introduced in this paper is based on the presence of small catalyst particles in the liquid film around a gas bubble, which results in a decreased effective film thickness and an increased k_L (see also [6–9]).

To study the effects of the two types of segregation phenomena (adhesion and agglomeration), the hydrogenation of methyl acrylate is used as a model reaction.

2. Experimental

2.1. Hydrogenation of methyl acrylate

A schematic representation of the glass slurry reactor used for our experiments is given in Fig. 1. This thermostatted stirred tank reactor is designed according to a standard geometry [10]. The catalysts used are 5 wt% Pd/Al_2O_3 and 10 wt% Pd/C (Fluka Chemie, AG) in a concentration range from γ_s=0.1 to 1 kg m^{-3} (see also Table 1). The concentration methyl acrylate in distilled water is varied between 0.06 and 0.19 mol l^{-1}. Hydrogen is used as the gas phase. All experiments are performed at atmospheric pressure and a stirrer speed of 6.67 s^{-1} (400 rpm). A typical experiment (C_{ma}=0.063 mol l^{-1}, γ_s=0.5 kg m^{-3}) is performed in the following way: the reactor is filled with 0.350 l distilled water, 2 ml methyl acrylate, and 0.17 g catalyst. The stirrer is started and the reactor is thermostatted at 303 K. Subsequently the reactor is degassed in vacuum. After degassing the reaction is started by filling the reactor with hydrogen. The hydrogen consumption is followed by using a graded tube sealed with a mercury ring.

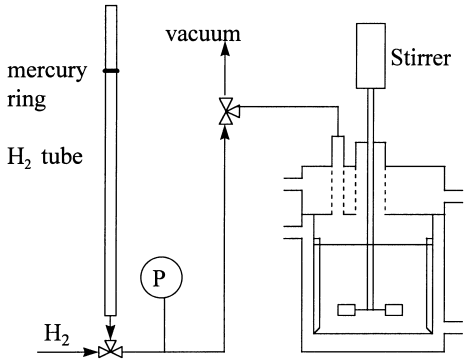

Fig. 1. Schematic representation of the stirred tank reactor.

Table 1
Physical properties of the catalysts used

Catalyst	Pd/C	Pd/Al_2O_3
Particle or agglomerate diameter, d_p (μm)	6.0±2.5	7.4±5.9
Density, ρ_{pg} (kg m^{-3})	1344	2148
Partition coefficient, m [8]	945	1520

2.2. Catalyst characterisation

Under equilibrium conditions, the distribution of the hydrogen between the particle and the liquid is described by a partition coefficient denoted as m. This parameter reflects the gas adsorption capacity of the solid particles and has been determined by Vinke et al. [8]. The average diameter of the particles or agglomerates, d_p, is determined with a Coulter Counter. The density of the catalyst particles is calculated from the densities of carbon and alumina, obtained from mercury porosimetry, and the known density of palladium. The values of these properties are given in Table 1.

A microscope is used to investigate agglomeration of particles under stagnant conditions. Five different solutions of methyl acrylate in distilled water are prepared: 0, 0.06, 0.09, 0.13, and 0.19 mol l^{-1}. An amount of 0.025 g Pd/C catalyst is dispersed in 10 ml of each solution. These samples are observed and photographed at an enlargement factor of 40.

3. Model development

Vinke et al. [1] reported that the adhesion of particles to bubbles in an aqueous solution is affected by the hydrophobicity of the catalyst. Hydrophobic particles show a higher bubble coverage than hydrophilic particles. In case of mass transfer limited reactions in aqueous solutions, the mass transfer of the reactant is enhanced as a result of the presence of the catalyst particles in the liquid film around gas bubbles. Therefore, the conversion rate increases for a higher bubble coverage. The mass transfer rate enhancement resulting from particle to bubble adhesion may be described by a model based on adhesion, film theory, and the following assumptions:

1. The particles are spherical and of equal size.
2. The value of the specific bubble surface, a_L, is not influenced by the particles present in the liquid phase.
3. Adhering particles are much smaller than the gas bubbles ($d_p<d_b$). Therefore, the interface between the particles and the bubble surface can be considered as being flat. In case of adhering particles the effective film thickness is reduced to half of the particle radius ($\delta_{eff}=d_p/4$) [8], therefore k_{LS} can be calculated by $k_{LS} = 4D_{AB}/d_p$.
4. The contribution of non-adhering particles (to small to enter the film layer) to the enhancement factor is negligible small.

In the presence of adhering particles, the bubble is partly covered with particles (Fig. 2).

In case of partly covered bubbles the mass transfer rate of the gaseous reactant is the result of a contribution from the mass transfer through the non-covered and through the covered part of the bubble, respectively (Figs. 2 and 3(a) and (b)).

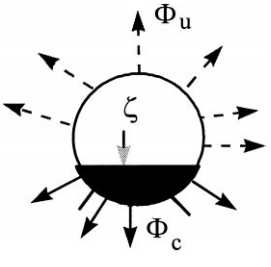

Fig. 2. Schematic representation of the gas–liquid interfacial mass transfer in case of a partly covered bubble (dashed arrows: through the uncovered part of the bubble, full arrows: through the covered part of the bubble).

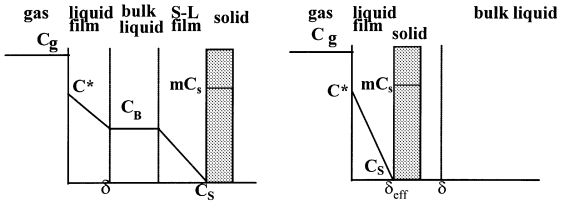

Fig. 3. (a) Mass transfer through uncovered part of bubble (Φ_u); (b) mass transfer through covered part of bubble (Φ_c).

The increase in the conversion rate under mass transfer limited conditions can be expressed in terms of an enhancement factor (E), defined as the ratio between the conversion rate in presence of adhering particles (Φ_ζ) and the conversion rate in absence of adhering particles ($\Phi_{\zeta=0}$). A proper calculation of E involves the use of similar hydrodynamic conditions and specific external catalyst surface area. The defining equations are:

$$E = \left[\frac{\Phi_\zeta}{\Phi_{\zeta=0}}\right], \tag{1}$$

in which

$$\Phi_\zeta = \zeta\Phi_c + (1-\zeta)\Phi_u, \tag{2}$$

$$\Phi_{\zeta=0} = \Phi_u. \tag{3}$$

Under the assumption that the conversion rate is determined by the film mass transfer of the gaseous reactant, one may derive the following equation for the mass transfer rate through the uncovered part of the bubble for a first order reaction:

$$\Phi_u = k_L a_L V_L (C^* - C_B) = k_s a_s V_L (C_B - C_s) = k_r \eta m V_L C_s \gamma_s / \rho_{pg}, \tag{4}$$

where $a_S = 6\gamma_S/d_p\rho_{pg}$, $k_s = 2D_{AB}/d_p$, and η is the effectiveness factor of the catalyst.

Elimination of C_B and substitution of a_S into Eq. (4) results in the following equation for the mass transfer rate through the uncovered part of the bubble.

$$\Phi_u = C^* V_L k_L a_L \Big/ \left(\frac{1 + k_L a_L \rho_{pg}}{\gamma_s}\left(\frac{d_p}{6k_s} + \frac{1}{k_r \eta m}\right)\right). \tag{5A}$$

In order to obtain the values of $k_L a_L$ and $k_r\eta$ from a plot of $(C^* V_L/\Phi_u)$ versus (ρ_{pg}/γ_s) Eq. (5A) may be reformulated as:

$$\frac{C^* V_L}{\Phi_u} = \frac{1}{k_L a_L} + \left(\frac{d_p}{6k_S} + \frac{1}{k_r \eta m}\right)\frac{\rho_{pg}}{\gamma_S}. \quad (5B)$$

For the covered part of the bubble the hydrogen flow rate is given by the following equation, using the assumption that $C_S \approx 0$, i.e. full mass transfer control [11]:

$$\Phi_c = k_{LS} a_L V_L C^*. \quad (6)$$

Substitution of Eqs. (2), (3) and (6) into Eq. (1) leads to the following relation between the enhancement factor, E, and the catalyst concentration, γ_s.

$$E = 1 + \zeta\left[\frac{k_{LS}}{k_L} + \frac{k_{LS} a_L \rho_{pg}}{\gamma_S}\left(\frac{d_p}{6k_S} + \frac{1}{k_r \eta m}\right) - 1\right]. \quad (7)$$

If we assume that the probability of collision with a gas bubble is equal for each individual particle we may derive the following collision probability function:

$$\Phi d(\gamma_S) = e^{-q\gamma_s} d(q\gamma_s). \quad (8)$$

The fraction ζ of the bubble covered by adhering particles as a function of the catalyst concentration γ_s can be obtained from:

$$\zeta = \int_0^{\gamma_s} \Phi d(\gamma_s) = \int_0^{\gamma_s} e^{-q\gamma_s} d(q\gamma_s) = 1 - e^{-q\gamma_s}. \quad (9)$$

For $\gamma_s \to \infty$ the fraction ζ becomes ζ_{max}, resulting in the following bubble coverage function:

$$\zeta = \zeta_{max}(1 - e^{-q(\gamma_s)}). \quad (10)$$

In Eq. (10) ζ_{max} represents the maximum bubble coverage for the specific three phases applied, which is observed at a high catalyst concentration in the slurry. ζ_{max} is a function of the hydrophobicity of the catalyst surface and the hydrodynamics in the reactor. However, below a critical catalyst concentration γ_{S0}, the number of adhering particles is assumed to be zero. This can be rationalised as below a certain catalyst concentration, particles do not adhere within a finite timescale. Taking into account this boundary condition, the following equation for the bubble coverage is obtained:

$$\zeta = \zeta_{max}(1 - e^{-q(\gamma_s - \gamma_{s0})}) \quad \text{for } \gamma_s > \gamma_{s0}, \quad (11)$$

$$\zeta = 0 \quad \text{for } \gamma_s < \gamma_{s0}. \quad (12)$$

The parameters q and γ_{S0} are constants which depend on the hydrodynamic conditions in the stirred tank reactor.

4. Results and discussion

Previous experiments in our laboratory concerning the hydrogenation of methyl acrylate showed that, under the conditions used for the work presented in this paper, the conversion rate is first order in hydrogen, independent of the methyl acrylate concentration and dependent on the stirring rate. These results show that this reaction is a hydrogen-mass transfer rate limited reaction.

4.1. Determination of the parameters k_L, a_L and $k_r\eta$

Vinke et al. [1] observed that, for an aqueous slurry, Pd/C particles strongly adhere to hydrogen bubbles while Pd/Al_2O_3 particles do not. Hence the conversion rate under mass transfer limited conditions in presence of Pd/Al_2O_3 particles represents the conversion rate at zero coverage $\Phi_{\zeta=0}$ (see Eq. (1)). The conversion rate measured in the current study for the hydrogenation of methyl acrylate to methyl propionate in presence of Pd/Al_2O_3 particles is shown in Fig. 4. The corresponding values of $k_L a_L$ and $k_r\eta$ for the Pd/Al_2O_3 system can

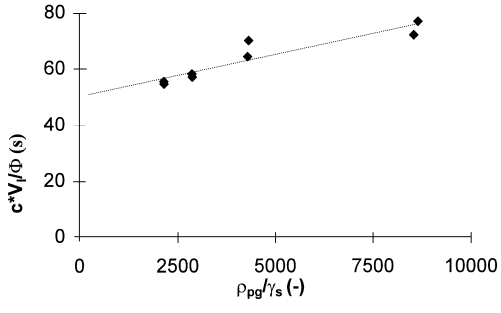

Fig. 4. $C^* V_L/\Phi_u$ versus ρ_{pg}/γ_s for the mass transfer limited hydrogenation of 0.6 mol l^{-1} in presence of Pd/Al_2O_3 catalyst particles (C^*=0.76 mol m^{-3}, C_{ma}=0.06 mol l^{-1}). The markers (◆) represent the experimental data, the solid line is the result of a best fit procedure Eq. (5B).

be obtained from the intercept and slope of a plot of $C^* V_L/\Phi_u$ versus ρ_{pg}/γ_s using Eq. (5B) (see Fig. 4).

From a best fit procedure we found the following values for $k_L a_L$ ($2.0\times10^{-2}\ s^{-1}$) and $k_r\eta$ ($0.38\ s^{-1}$). The observed gas hold-up ϵ and bubble diameter d_b are 0.01–0.015 and 1.5×10^{-3}–2×10^{-3} m respectively. This results in an approximate value for a_L of $40\ m^2\ m^{-3}$ ($a_L = 6\epsilon/d_b$).

In the following sections the influence of the Pd/C catalyst concentration and methyl acrylate concentration on the enhancement factor in case of the hydrogenation of methyl acrylate to methyl propionate will be presented.

4.2. Effect of catalyst concentration

Fig. 5 shows the experimental results for the enhancement factor as a function of the catalyst concentration, as calculated by Eq. (1) in which Φ_ζ is the measured conversion rate of methyl acrylate in presence of a Pd/C catalyst and $\Phi_{\zeta=0}$ is derived from the measured conversion rate in presence of a Pd/Al_2O_3 catalyst for the same value of the specific external catalyst surface. The concentration methyl acrylate is $0.06\ mol\ l^{-1}$ for all experiments. The solid line through the markers is calculated using Eqs. (7), (11) and (12) after substitution of the appropriate values of ζ_{max}, q, and γ_{S0} (see Table 2) obtained from a best fit procedure. From the experimental data represented in Fig. 5 it can be seen that the value of γ_{S0} lies in a small interval with the boundary values 0.07 and $0.078\ kg\ m^{-3}$. From flotation experiments

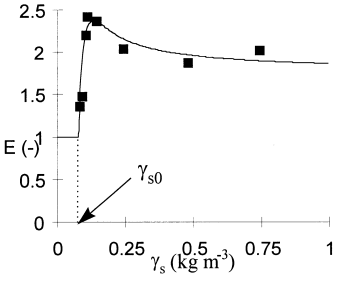

Fig. 5. The enhancement factor E as a function of the catalyst concentration γ_s: (■) ratio of the experimental conversion rates in presence of Pd/C particles and the experimental conversion rate in the presence of Pd/Al_2O_3 particles as defined by Eq. (1). The solid line is calculated from Eqs. (7), (11) and (12) using the values of ζ_{max}, q, and γ_{S0} as in Table 2.

Table 2
The values of ζ_{max}, γ_{S0}, and q obtained by a best fit procedure of the data points in Fig. 5

Parameter	Value
ζ_{max}	0.2
γ_{S0} ($kg\ m^{-3}$)	0.075
q ($m^3\ kg^{-1}$)	46

under non-stagnant conditions (to be published) ζ_{max} was found to range between 0.1 and 0.25. This value of ζ_{max} is in good agreement with the value obtained by a best fit procedure (Table 2).

4.3. Impact of the methyl acrylate concentration on catalyst agglomeration

Under stagnant hydrodynamic conditions the agglomerate size of Pd/C catalyst particles decreases for higher methyl acrylate concentrations (Fig. 6). The captions in this figure also give the surface tension σ_{LG} of the liquid phase.

The agglomeration behaviour of Pd/Al_2O_3 is also investigated by microscopic imaging, but no significant change in agglomeration is observed. If a similar agglomeration behaviour of both catalysts occurs under non-stagnant reactor conditions an increase of the conversion rate with increasing concentration methyl acrylate is expected due to the decreasing effective particle diameter. The results of the hydrogenation of methyl acrylate at different methyl acrylate concentration are presented in Fig. 7. This figure clearly shows the expected increase of the conversion rate for increasing concentration methyl acrylate.

Under the assumption that the increased conversion rate at increasing concentrations methyl acrylate is only caused by de-agglomeration, so by a decreasing effective particle diameter, Eq. (2) can be used to calculate this effective catalyst particle diameter d_{eff}. The result of this calculation is given in Table 3 and Fig. 8.

In order to obtain the enhancement factor E, the value of Φ_{Pd/Al_2O_3} is calculated at the specific external catalyst surface for the different effective catalyst particle diameters (see Table 3). The enhancement factor obtained in this way and the corresponding effective particle diameters are plotted in Fig. 8. The solid line represents the enhancement factor

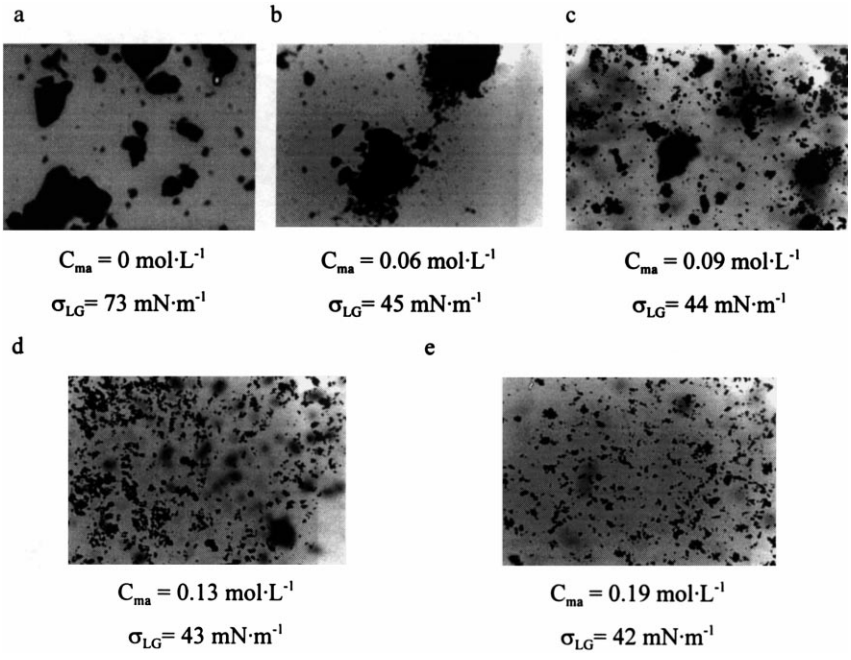

Fig. 6. Microscopic images (125×200 μm) of Pd/C slurry for different methyl acrylate concentration (C_{ma}) in water and the corresponding surface tension σ_{LG} of the liquid phase.

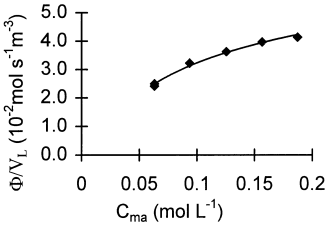

Fig. 7. The conversion rate for the hydrogenation of methyl acrylate under mass transfer limited conditions as a function of methyl acrylate concentration (γ_s=0.5 kg m^{-3}).

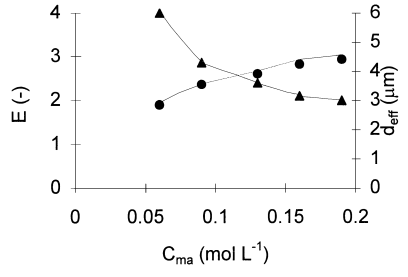

Fig. 8. The enhancement factor E, and the effective particle diameter d_{eff}, as a function of the methyl acrylate concentration (γ_s=0.5 kg m^{-3}, ζ_{max}, γ_{S0}, and q (see Table 2)): (●) the measured value of E; (———) the model; (▲) the calculated values of d_{eff} (right-hand axis).

Table 3
The calculated effective particle diameter under non-stagnant conditions for various methyl acrylate concentrations (γ_s=0.5 kg m^{-3}, ζ_{max}, γ_{S0}, and q (see Table 2))

C_{ma} (mol l^{-1})	d_{eff} (μm)
0.06	6.0
0.09	4.3
0.13	3.6
0.16	3.2
0.19	3.0

calculated from Eqs. (7), (11) and (12) and the appropriate values of ζ_{max}, q, and γ_{S0} (Table 2) using the values of the effective particle diameter at the various methyl acrylate concentrations.

Several possible explanations for the observed increase in conversion rate as a function of the concentration methyl acrylate could be put forward, e.g. an increasing specific bubble surface and a change in

the bubble coverage. For the surface tensions used for our experiments the change in the specific bubble surface will not exceed 5% [12], which cannot explain the change in the conversion rate. Fig. 8 shows that the observed increased enhancement can be explained by a decreasing effective particle diameter. Therefore, the authors believe that the agglomeration behaviour of the catalyst particles is an important reason for the observed enhancement. This hypothesis is supported by the fact that the calculated values of the effective particle diameter under non-stagnant reactor conditions, represented in Table 3, show a similar trend with the concentration as the agglomerates under stagnant hydrodynamic conditions represented in Fig. 6. This effect of methyl acrylate on agglomeration can be caused by three different phenomena. The first possible explanation is the effect of the surface tension. The other two possible explanations are both based on adsorption of methyl acrylate on the catalytic surface: i.e. an effect on hydrophobicity and on the interparticle forces. The results represented in Fig. 6 show that the decreasing degree of agglomeration is not a function of the surface tension. The effect of adsorption of methyl acrylate on agglomeration needs to be investigated.

5. Conclusions

A model is developed which describes the enhancement of the conversion rate of the hydrogenation of methyl acrylate caused by an increase in hydrogen transfer rate due to adhesion of catalyst particles to gas bubbles. This model is based on the gas–liquid film theory, particle to bubble collision probability and the effect of the particle diameter of adhering particles on the effective film thickness.

The enhancement factors E obtained from hydrogenation experiments at different catalyst concentrations (γ_S=0.1–1 kg m^{-3}) and several methyl acrylate concentrations (C_{ma}=0.06–0.19 mol l^{-1}) are in excellent agreement with the results of the introduced model.

An important phenomenon is the agglomeration of Pd/C catalyst particles. A decrease in agglomerate size with increasing concentration of methyl acrylate is observed under both stagnant and is likely to hold under non-stagnant conditions, resulting in an increased conversion rate and enhancement factor. The agglomeration behaviour of the Pd/C catalyst particles cannot be explained by an effect of the surface tension of the liquid phase.

6. Nomenclature

a_L	bubble surface per unit of slurry volume (m^2 m^{-3})
a_S	external catalyst surface per unit of slurry volume (m^2 m^{-3})
C_g	concentration of the gaseous reactant in gas phase (mol m^{-3})
C^*	concentration at the film side of the gas–liquid interface (mol m^{-3})
C_B	concentration of the gaseous reactant in the bulk liquid (mol m^{-3})
C_S	concentration of the gaseous reactant at the liquid side of the solid–liquid interface (mol m^{-3})
C_{ma}	concentration methyl acrylate (mol l^{-1})
D_{AB}	binary diffusion coefficient (m^2 s^{-1})
d_p	particle diameter (m)
E	Enhancement factor (dimensionless)
k_L	liquid-side mass transfer coefficient for the uncovered part of the bubble surface (m s^{-1})
k_{LS}	liquid-side mass transfer coefficient for the covered part of the bubble surface (m s^{-1})
k_S	mass transfer coefficient from the bulk liquid to the surface of the catalyst (m s^{-1})
k_r	reaction rate constant (s^{-1})
m	partition coefficient defined as the ratio between the amount of gas phase reactant molecules per unit volume catalyst and the amount of gas phase reactant molecules per unit volume liquid (dimensionless)
q	constant used in Eq. (11) (m^3 kg^{-1})
V_L	volume of the solid–liquid suspension in the reactor (m^3)

Greek symbols

ϵ	gas hold-up, volume gas per total volume of suspension and gas (m^3 m^{-3})
δ	liquid-film thickness at the uncovered part of the bubble (m)
δ_{eff}	effective liquid-film thickness at the covered part of the bubble (m)

Φ collision probability function (dimensionless)
Φ_c gaseous mass transfer rate for the covered part of the bubble (mol s^{-1})
Φ_u gaseous mass transfer rate for the uncovered part of the bubble (mol s^{-1})
Φ_ζ conversion rate in presence of adhering particles (mol s^{-1})
$\Phi_{\zeta=0}$ conversion rate in absence of adhering particles (mol s^{-1})
γ_S catalyst concentration in the slurry (kg m^{-3})
γ_{S0} critical catalyst concentration (kg m^{-3})
η effectiveness factor of the catalyst (dimensionless)
ρ_{pg} density of a dried catalyst with gas filled pores (kg m^{-3})
σ_{LG} static surface tension between gas phase and liquid phase (N m^{-1})
ζ fraction of bubble surface covered by adhering particles (dimensionless)
ζ_{max} maximum bubble coverage (dimensionless)

References

[1] H. Vinke, P.J. Hamersma, J.M.H. Fortuin, AIChE J. 37 (1991) 1801.
[2] D. Lindner, M. Werner, A. Schumpe, AIChE J. 34 (1988) 1691.
[3] E. Alper, B. Wichtendahl, W.-D. Deckwer, Chem. Eng. Sci. 35 (1980) 217.
[4] R.L. Kars, R.J. Best, A.A.H. Drinkenburg, Chem. Eng. J. 17 (1979) 201.
[5] G. Quicker, E. Alper, W.-D. Deckwer, AIChE J. 33 (1987) 871.
[6] S.K. Pal, M.M. Sharma, V.A. Juvekar, Chem. Eng. Sci. 37 (1982) 327.
[7] R.D. Holstvoogd, W.P.M. van Swaaij, Chem. Eng. Sci. 45 (1990) 151.
[8] H. Vinke, P.J. Hamersma, J.M.H. Fortuin, Chem. Eng. Sci. 48 (1993) 2197.
[9] C. Joly Vuillemin, C. de Bellefon, H. Delmas, Chem. Eng. Sci. 51 (1996) 2149.
[10] S.E. Forrester, C.D. Rielly, Chem. Eng. Sci. 49 (1994) 5700.
[11] K.R. Westerterp, W.P.M. van Swaaij, A.A.C.M. Beenackers, Chemical Reactor Design and Operation, Wiley, 1993, p. 434.
[12] R.H. Perry, Perry's Chemical Engineerings' Handbook, McGraw-Hill, Singapore, 1984, pp. 18–68.